Electrode and Ground Arrangement on Sample Plate Under Electrostatic Powder Coating Process

Colonel Professor Dr. Suwimon Saneewong Na Ayuttaya

Department of Mechanical Engineering, Academic Division,
Chulachomklao Royal Military Academy, Nakhon Nayok 26001, Thailand
Corresponding Author. E-mail : joysuwimon1@hotmail.com
(Received: April 4, 2024, Revised: May 19, 2024, Accepted: May 23, 2024)

Abstract : In this research study, the electrode and ground arrangement on sample plate is studied in order to increase the electrostatic powder coating process. The electrode and ground arrangement are varied in order to improve the electric force and the thickness of coating. The first result shows the electric force is appearing under the electrostatic process, and the electrical voltage distribution is different with various the electrode and ground arrangement. For the second part, the thickness of the powder coating of the sample plate is increased with the number of the coating, and the electrostatic process can more increase the thickness of coating than without the electrostatic process. In addition, the electrode and ground arrangement are affected with the thickness of the powder coating on the sample plate. In the last part, a similar trend of the graph has appeared in the experimental and the numerical results, so the experimental results have good agreement with the experimental results.

Keywords : Electrostatic Process, Powder Coating, Sample Plate, Electrode and Ground Arrangement

1. Introduction

Coating process is the one process for transferring a liquid onto a material. The coating process consists of applying a coating material to a moving web of the flexible substrate. The coating material may be paper, acrylic, or aluminum foil and the resulting material's additional properties will vary depending on the required application [1-3]. The benefit of coating is that it delivers to the substrate enhanced aesthetic and physical properties derived from the coating material. Industrial coatings play vital roles in protecting military vehicles and military aerospace coating material. The military coating applications help protect against the damage caused by wear-prone applications. In addition, they have been designed to be wearing resistant, reduce friction, reduce corrosion and abrasion or heat [4-5]. The combination of the coating process and different techniques is systematically studied in order to improve the coating process efficiency.

The physical vapor deposition process, chemical vapor deposition process, sol-gel coating, thermal spray coating, and electrostatic powder coating process are the type of the deposition process. The physical vapor deposition process refers to a variety of thin film deposition techniques where a solid material is vaporized in a vacuum environment and deposited on substrates as a pure material or alloy composition coating [6]. The chemical vapor deposition is a process that involves the reaction of a volatile precursor which is injected into a chamber. By the chamber is under vacuum and it is heated to a reaction temperature that causes the precursor gas to react or break down into the desired coating and bond to the material surface [7]. The sol-gel coating involves the hydrolysis and condensation of alkoxide precursor water to form a colloidal dispersion of particles [8]. The thermal spray coating is a process that sprays coating materials using the pressure of a high-heat gas. The material then bonds to the surface, forming a coating that corrosion protection, thermal resistance, environmental protection, lubricity, wear resistance and electrical and thermal conductivity [9]. The electrostatic powder coating process is a process by which electrically charged particles are deposited out of a water suspension to coat a conductive part. During the electrostatic process, paint is applied to a part at a certain film thickness, which is regulated by the amount of voltage applied [10].

Behzad et al. [11] showed a literature review of the coating techniques for surface protection. The coating processes were reliable means of material deposition and surface protection, but there were advantages and disadvantages to all of them in different applications. The physical vapor deposition process could cause corrosion and wear resistance. The thin film deposition could have adjustable mechanical, corrosion, and aesthetic properties. But this deposition process required a high vacuum, and the corrosion resistance was affected by abrasion. The chemical vapor deposition process could cause corrosion and wear resistance. It could be coated by the deposition of various types of materials with different microstructures. In addition, the coating materials could work at low atmospheric pressures. But the material could be heat-resistant. The sol-gel coating was cost- effective in biomedical applications. It could provide corrosion and ion release protection. The material could have high adhesion in the multilayered coating process. But this process was restricted by the thickness control and the slow rate of the coating cycle. The failure during heat treatment was the possibility of coating multilayered structures. For the thermal spray coating, the material was non-conductive and had corrosion and wear resistance. But it had several disadvantages, such as requiring a small range of powder sizes with a narrow size distribution, numerous process variables to change the coating structure, and a heat source. There have several advantages to the electrostatic powder coating process, such as high corrosion resistance and hardness, porous structure for biomedical applications, low-corrosion and wear, and high-temperature applications. This coating was suitable for valve metals and could be used for conductive substrates.

Some researchers are studying the electrostatic powder coating process [12-16]. Sharmene et al. [12] studied the trajectories of charged powder particles in an electrostatic powder coating system. The mathematical model was modeled considering electrical and fluid forces in order to computed charge density in the gun-to-target region. The simulation results showed good agreement with experimental data at several collection points on the painting target and provided valuable information concerning particle deposition. Schmitt and Lebienvenu [14] studied the conductive polymeric materials used for electrostatic painting applications. The critical volume fraction of fibres and give its valued for a little fibre–matrix associations were investigated. The result shown that the microstructure had a strong effect on the overall mechanical properties of the composite material. Toljic et al. [15] studied the three-dimensional FLUENT numerical model of the electrostatic coating process for the automotive industry. The result shown that the transfer efficiency increases when the electrical forces and that the coating uniformity improved with the movement of the target.

The electrostatic powder coating process is the process by which a positively charged electron within the spray nozzle charges the paint particles. These particles all have a positive charge; they repel each other and break apart, resulting in a fine mist that coats evenly. There is also a magnetic field effect, and the negative charge of the workpiece attracts the positive charge of the paint particles across its full surface. For this result, the electrostatic powder coating process is used in this research in order to produce automotive grade spray paint that can be used on vehicles and military aerospace coating materials. For this result, the electrostatic powder coating process is used in this research in order to be cost effective in military vehicles and military aerospace. In the previous study, it was not systematically studied. In this study, the mechanism of the electrostatic powder coating is seriously investigated for the coating process. The effect of the electrode and ground arrangement on the sample plate is systematically proposed in order to improve the powder coating process. The first part, the electric force is numerically studied under the electrostatic process. The second and third parts are experimental studies of the powder coating on the sample without and with the electrostatic process, respectively. The verification and problem statements are analyzed in the last part.

2. Governing equation

The electrostatic process is a branch of physics that directly converts electrical energy into kinetic energy without mechanical pieces. The influence of electrostatic phenomena can change the pattern of fluid flow and enhances transport phenomena with lowering energy supplied [17]. From the mechanism and characteristic of the electrostatic process, Saneewong Na Ayuttaya [18] divided the fourth group of applications. The first group was increasing flow mechanism; it was used for pumping and biomechanics application. The second group was injection flow mechanism; it was used for the droplet, electrospray and microfluidics. The third group was inducing flow mechanism; it was used for electrostatic precipitator and actuator. The last group was mixing particle process; it was used for boiling and condensation, heat and mass transfer, heat exchanger and drying process. For the third group (inducing flow mechanism), the induced flow caused the total reaction to lean backward in the plane of rotation. This also reduced the perpendicular component of the total reaction and reduced total rotor thrust. The motion and precipitation of dust particles in an electrostatic precipitation depended on the electric field, space charge, and gas flow field and dust particle properties. The electrostatic coating is used for inducing flow mechanism in order to increase the adhesion of powder painting [19].

The governing equations for the electric force per unit volume f_E (Eq. (2.1)) generated by the electric fields with strength E in airflow of dielectric permittivity (ε), density (ρ), and uniform temperature (T) [20]. Electric field distribution is computed by using Maxwell's equations (Eqs. (2.2)-(2.5)) listed as below:

$$\vec{f}_E = q\vec{E} - \frac{1}{2}\vec{E}^2\nabla\varepsilon + \frac{1}{2}\nabla\left[\vec{E}^2\left[\frac{\partial\varepsilon}{\partial\rho}\right]_T\rho\right], \tag{2.1}$$

$$\nabla \cdot \varepsilon\vec{E} = q, \tag{2.2}$$

$$\nabla \cdot J + \frac{\partial q}{\partial t} = 0, \tag{2.3}$$

$$J = qb\vec{E} + q\vec{v}, \tag{2.4}$$

(2.5)

This electric energy density (η_E) can be used to calculate the energy stored in a electric field, as shown in Eq. (2.6).

$$\eta_E = \varepsilon E^2 \tag{2.6}$$

where v is flow velocity, q is the space charge density in the fluid, V is electrical voltage, J is current density, and t is time. The ion mobility (b) is 1.80 x 10^{-4} m^2/V.s and the dielectric permittivity of free space (ε) is 8.85 x 10^{-12} F/m.

From Eq. (2.1), three terms are theelectrophoretic, dielectrophoretic, and electrostrictive forces, respectively. In the first term, the electrophoretic force results from the net uncharged within the fluid or ions injected from the electrodes. Electric field distribution is emitted from the electrode and induces to the ground. The second term, the dielectrophoretic force is a consequence of inhomogeneity in the permittivity of the dielectric fluid due to the non-uniform electric field, temperature gradients, and phase differences. The last term, the electrostrictive force is caused by non-homogeneous electric field strength and the variation in dielectric constant with temperature and density [21].

The governing equations are developed to predict the flow field. The continuity and Navier-Stokes equations which are coupled with the Coulomb force equation are considered from Eqs. (2.7) and (2.8), respectively. They are expressed by:

$$\nabla \cdot \vec{v} = 0, \tag{2.7}$$

$$\rho\left[\frac{\partial \vec{v}}{\partial t} + (\vec{v} \cdot \nabla)\vec{v}\right] = -\nabla\vec{P} + \mu\nabla^2\vec{v} + \vec{f}_E \tag{2.8}$$

where μ is viscosity and P is pressure.

The heat and mass transfer in sprays has been measured with the convective heat transfer coefficient (h_c) (Eq. (2.9)) and the Sherwood number (Sh) (Eq. (2.10)), respectively. Convective heat transfer is the movement of thermal energy within fluids, and the Sherwood number is a dimensionless number used in mass transfer operations. It represents the ratio of the total heat and mass transfer rate to the rate of diffusive transport. The mass transfer rate is composed of convection and diffusion.

$$h_c = -\frac{k}{\Delta T}\frac{\partial T}{\partial n}, \tag{2.9}$$

$$Sh = \frac{\dot{m}}{\Delta C\, A_C}\frac{d}{D} \tag{2.10}$$

where k is thermal conductivity, n is coordinate in x and y axis, $\dot{m}$ is mass transfer rate, d is diameter of electrode, D is mass diffusivity, A_C is surface area of sample that is exposed to electrostatic powder coating process and ΔC is difference in water vapor concentration between the sample surface and ambient.

3. Method and model

For the electrostatic process, the electrode and the ground arrangement are varied on the sample plate. The experimental and numerical are investigated both of techniques. In this electrostatic powder coating process, the collected data of powder spray is investigated three times and an average score is used for these experimental results. The arrangement of the electrode and ground is very important in the electrostatic powder coating process. The pin of the electrode and ground are suitable for local heat transfer coefficient and the electrode and ground plate are suitable for average total heat transfer coefficient. The diagram of the electrode and ground arrangements above the sample plate are varied for seven patterns, as shown in Fig. 1. The symbol of electrode and ground is E in red color and G in blue color, respectively. The copper wire and copper plate are shown in yellow color. All of patterns are described in Table 1. After experimental analysis, the thickness of coating is measured by the cross-cut tester. The cross-cut tester uses a blade to cut through the coating to the substrate.

The spray paint is used the automotive grade spray paint formulated by concentrated lacquer. The premium color spray can be used on vehicles and military aerospace coating material. It is good quality paint which build beautiful film with glossy, durability, quick drying and good adhesion. The black paint material has solid fraction 72.34%. The wet and the dry density are 1.32 and 1.69 g/ml, respectively. The pressure supply is 200 bars, corresponding to a paint the mass flow rate of 0.02733 kg/s. The effective orifice diameter is 0.48-0.53 mm and spray angle are 45o. The gun to target distance is 300 mm and the booth air velocity is 0.1 m/s.

The coating parameters which should be observed during the coating operation such as the inlet and outlet air temperature, the outlet butterfly valve, the humidity Level, the tablet bed temperature, the spray rate and the atomizing air pressure.

Table 1 The data of the conventional coating (without electrostatic coating) and electrode and ground arrangements above the sample plate

Number of patterns	Fig.	Electrode Arrangement	Ground Arrangement
1	1 (b)	Electrode Wire in Square Arrangement	Ground Point
2	1 (c)	Electrode Wire in Circle Arrangement	Ground Point
3	1 (d)	Electrode Wire in Straight Line Arrangement	Ground Wire in Straight Line Arrangement
4	1 (e)	Electrode Wire in Circle Arrangement	Ground Wire in Straight Line Arrangement
5	1 (f)	Electrode Plate	Ground Plate
6	1 (g)	Electrode Wire in Square Arrangement	Ground Wire in Circle Arrangement
7	1 (h)	Electrode Wire in Square Arrangement	Ground Point

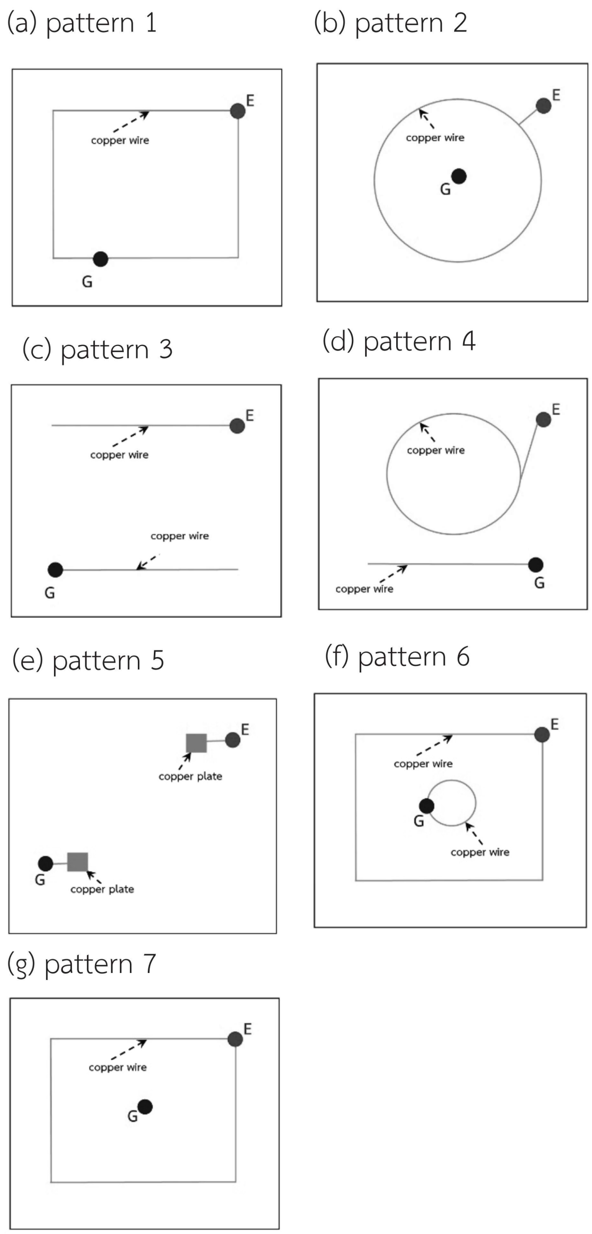

Fig. 1 The diagram of electrode and ground arrangements under the electrostatic powder coating process (a) pattern 1 (b) pattern 2 (c) pattern 3 (d) pattern 4 (e) pattern 5 (f) pattern 6 (g) pattern 7

The heat and mass transfer enhancement technique utilizing electrostatic process generated from the polarization of dielectric fluid. It can be one of the most promising methods among various active techniques because of its several advantages. This technique deals with the interdisciplinary field with subjects concerning the interactions between electric and flow fields. When an electrical voltage is exposed to airflow, ions from a sharp electrode move forwards to the ground. An ionic wind or primary flow is formed when air ions are accelerated by an electric field and exchange momentum with neutral air molecules. As a result, the momentum of airflow is enhanced.

3.1 Experimental analysis

The three-dimensional model for the powder coating is shown in Fig. 2. For the experimental analysis, the sample plate is mostly made of acrylic plate (the dimension of the sample plate is 15 x 15 cm^2). In order to study the electrode and ground arrangement, the electrode and the ground are made of copper, and they stick above the sample plate. The high voltage power supply (ACOPIAN model: NO30HP2M.-230) is used to create electrical voltage. and the copper is used to connect the circuit with the electrode and ground. The gap of the electrode and ground is in range 2-10 cm. Because the brake-down spark appears when the gap is less than 2 cm and the electrostatic process is not influenced when the gap is higher than 10 cm.

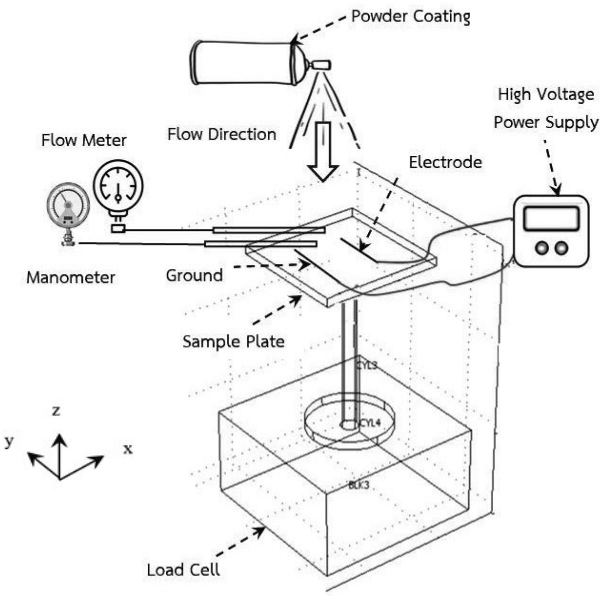

Fig. 2 Three-dimensional model for experimental setup

The flow meter and manometer are set up in order to meter the impact of airflow under the electrostatic powder coating process. The digital pressure manometer and the digital flow meter have an accuracy + 0.1 hPa + 1.5% and + 3% + 0.1 dgts, respectively. In each test run, impact pressure (P), impact velocity (v) and gravity force (F) under the electrostatic powder coating process is measured by a manometer, flow meter and load cell with data logger, respectively.

3.2 Numerical analysis

This electrostatic process deal to the interdisciplinary field with subjects concerning the interactions between the electric field and flow field. In this numerical analysis, the computational models are shown in Fig. 3 and compose of main two parts: the first and second parts are electric field model and flow field model, respectively. The dimensions of the three-dimensional model are 15 x 15 x 20 cm^3 and the dimensions of sample plate are 15 x 15 cm^2. The radius of circle electrode and circle ground are 0.1 cm. The space charge density (q_0) at the tip of the electrode is considered from Griffiths [20].

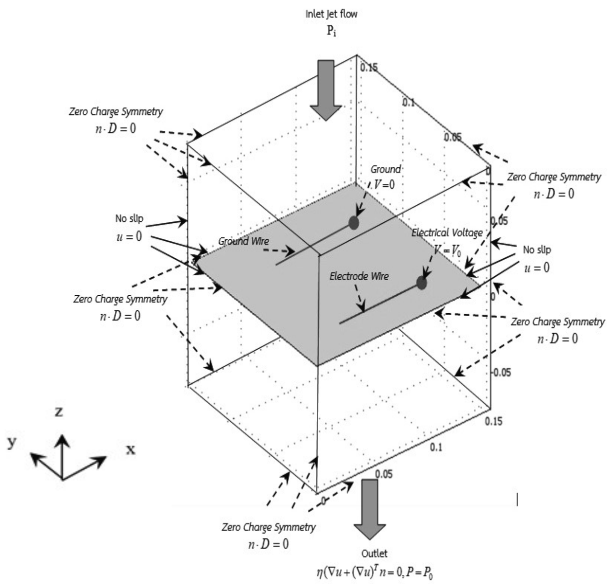

Fig. 3 The boundary condition for numerical analysis

For the boundary conditions for solving the electric field and flow field, the normal font and the Italics font for the boundary conditions are set for the electric field and flow field, respectively. The outer sides of the electric flow and sample plate boundary condition are considered as zero charge symmetry.

$$\mathrm{n} \cdot \mathrm{D} = 0 \tag{3.1}$$

where n is the outward normal from medium and D is electric flux density.

The tip of the electrode and ground are considered as electrical voltage and ground boundary condition, respectively.

$$V = V_0, \quad (3.2)$$

$$V = 0, \quad (3.3)$$

where subscript zero means at electrode wire. The inlet jet is inlet pressure (P_i) and the pressure of outlet boundary condition is considered with no viscous stress. This boundary condition specifies vanishing viscous stress along with a Dirichlet condition on the pressure:

$$\eta(\nabla\vec{u} + (\nabla\vec{u})^T \cdot n = 0 \text{ and } \vec{P} = \vec{P}_0, \quad (3.4)$$

where P_0 is atmospheric pressure, is kinematics viscosity and T is matrix transpose. All of the boundary and the sample plate are considered as no slip boundary condition. This is the standard and default boundary condition for a stationary solid wall. The condition prescribes:

$$\vec{u} = 0, \quad (3.5).$$

In this idea, a finite-dimensional space of some solutions and a number of points in the boundary and the collocation points are used for the given equation. This convergence test leads to a mesh having approximately 15,000 elements. A fine mesh is specified in the sensitive areas is discretized using a triangular element. With percentage error is lower than 0.1 and a dimensionless time step of 1 x 10^{-4} to ensure numerical stability and accuracy. The system of governing equations is solved with the unsymmetrical multi-frontal method. It is reasonable to assume that, in this element number, the accuracy of the simulation results is independent of the number of elements.

4. Results and discussion

The effect of the electrode and ground arrangement on the sample plate is systematically proposed in order to the powder coating process improvement. In this experimental study, the saturation vapor pressure is 0.0028-0.0031 bar, the relative humidity is 58-62% and the temperature of the condition experimental setup are controlled at 25^{O}C. The electrical voltage (V_0) is fixed at 20 kV and the inlet jet of powder coating is set at P_i = 490.33 kPa. For the first part, the electrode and ground arrangements under the electrostatic powder coating process are numerically varied in 7 patterns. The maximum electric field, the maximum electric energy density and the maximum surface charge density are investigated. For the second part, the powder coating from the electrostatic process is experimentally compared with the powder coating without the electrostatic process. The verification and problem statements are analyzed in the last part. The impact pressure ratio, the impact velocity ratio and the gravity force ratio of powder coating is varied in the electrode and the ground arrangement.

4.1 Numerical study the electric force under the electrostatic process

An electric field is the physical field that surrounds electrically charged particles and exerts force on all other charged particles in the field. The electric field is originated from electric charges, and it moved toward at the ground [22]. For the conventional coating process, the electrical voltage and the electric field distribution is not numerical appeared, as shown in Fig. 4. The electric field is appeared under the electrostatic process. The diagram from Fig. 1 is used in order to numerical studied the electrical voltage distribution, as shown in Fig. 5. In all the cases, the maximum electrical voltage is appeared at the tip of the electrode and the high value of electrical voltage is appeared in the electrode area. The zero electrical voltage is appeared at the ground area. The maximum and the minimum electrical voltage are not different for each arrangement. The electrical voltage distribution due to the different electrode and ground arrangement from Fig. 1 (a-g) has been already shown in Fig. 5 (a-g), respectively.

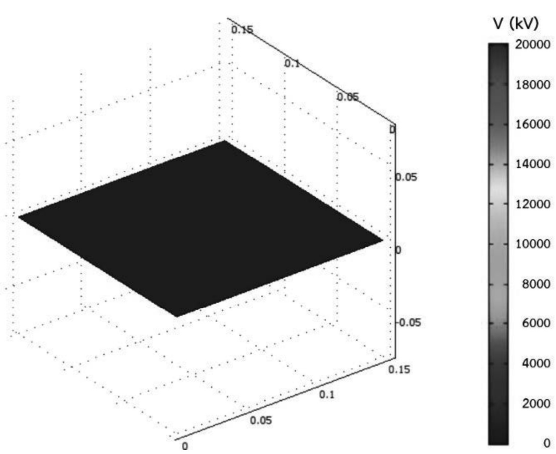

Fig. 4 Numerical results of conventional coating Process

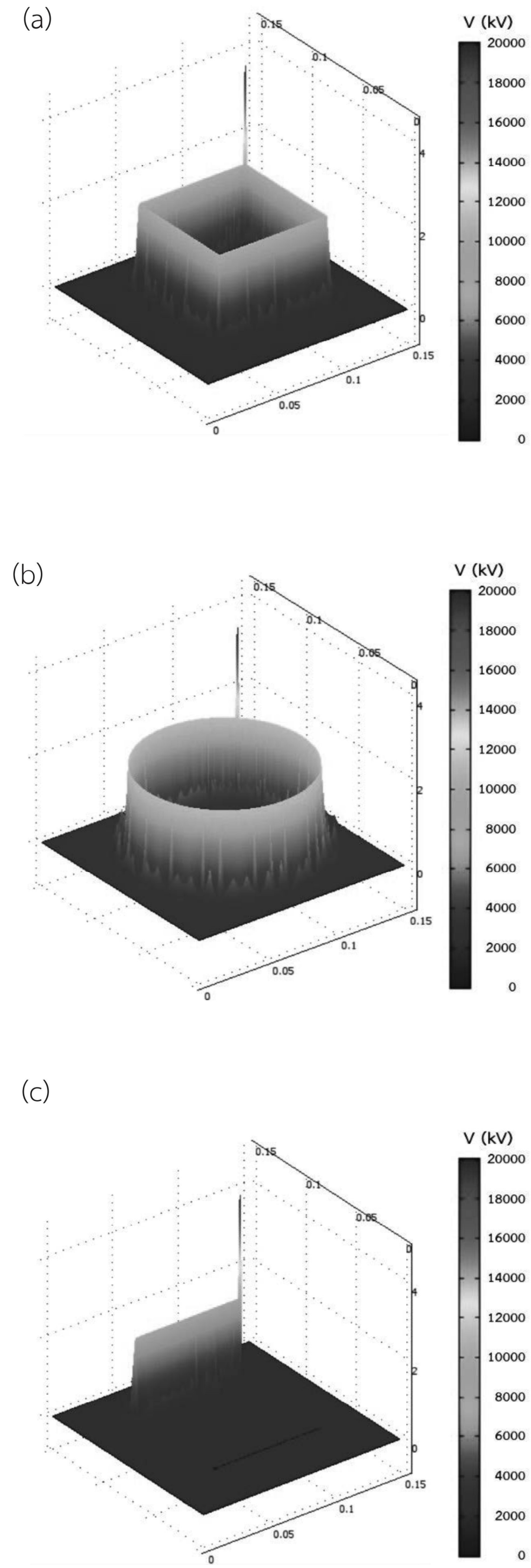

(d)

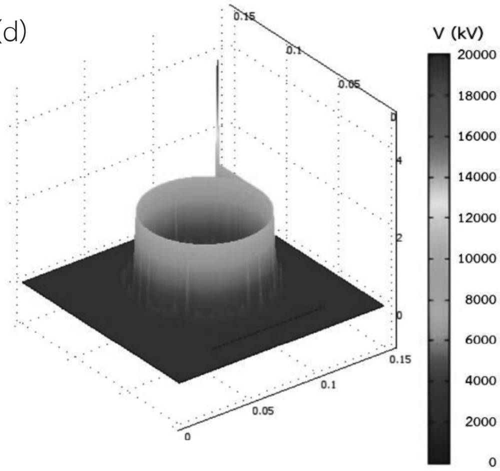

(e)

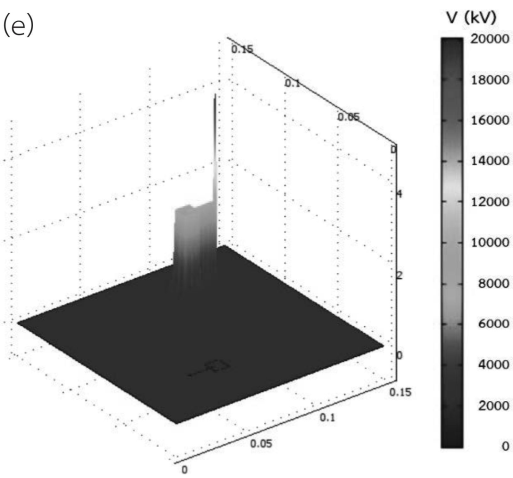

(f)

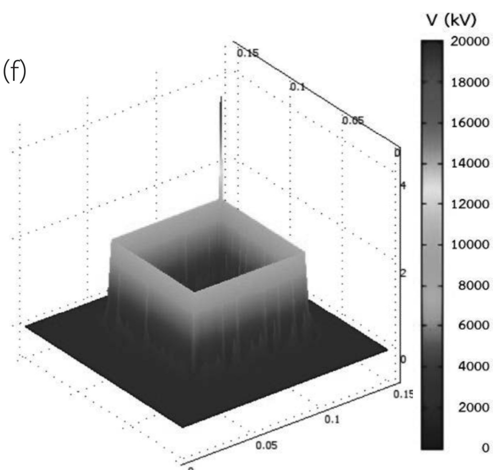

(g)

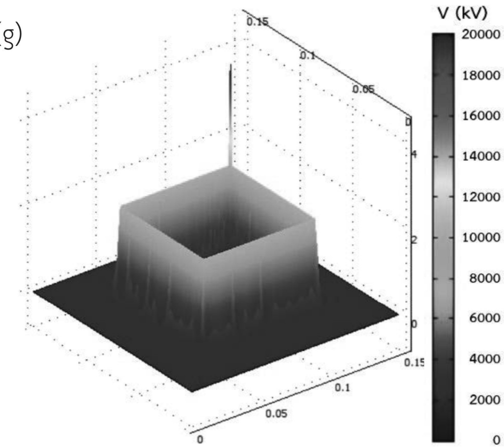

Fig. 5 Numerical results of electrical voltage distribution (a) pattern 1 (b) pattern 2 (c) pattern 3 (d) pattern 4 (e) pattern 5 (f) pattern 6 (g) pattern 7

In various the electrode and the ground arrangement with electrostatic process, the maximum electric field, the maximum electric energy density and maximum surface charge density are numerical investigated in Fig. 6-8, respectively. The maximum value in each case is not difference due to the electrical high voltage is fixed. It can be seen that the highest value of the electrode and the ground arrangement is the pattern 2 (electrode wire in circle arrangement and ground point) and pattern 3 (electrode and ground wire in straight line arrangement). The lowest value of the electrode and the ground arrangement is pattern 1 (electrode wire in circle arrangement and ground point). The maximum electric field, the maximum electric energy density and maximum surface charge density are affected to the electric force so electrostatic coating process increasing.

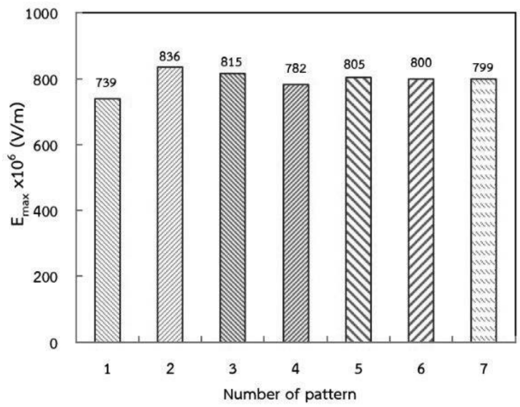

Fig. 6 The maximum electric field in various electrode and the ground arrangement with electrostatic process

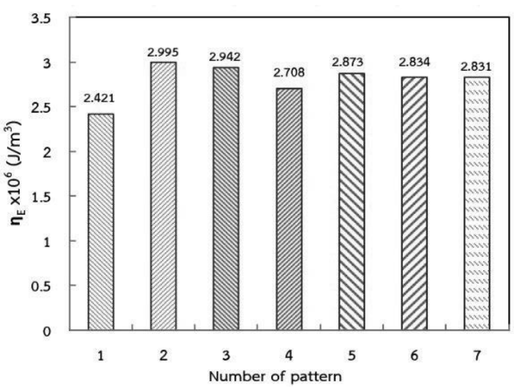

Fig. 7 The maximum electric energy density in various electrode and the ground arrangement with electrostatic process

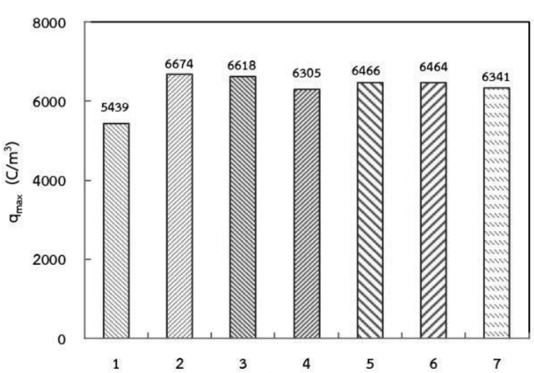

Fig. 8 The maximum surface charge density in various electrode and the ground arrangement with electrostatic process

4.2 Experimental study the powder coating on the sample without the electrostatic process

In this without electrostatic powder coating process, the powder coating is paint until 1-5 layers and it is waiting for 10 minutes in each layer. The collected data of powder spray are investigated three times, and an average score is used for these experimental results. Fig. 9 shows the powder coating on the sample without the electrostatic process. The thin layer and the little thick layer are appeared when coating process is 1 layer and 2 layers, as shown in Fig. 9 (a) and 9 (b), respectively. The thickness of coating is measured by the cross-cut tester. The thick layer is coated in case of the powder coating is 3 layers (Fig. 9 (c)) and 4 layers (Fig. 9 (d)). For 5 layers (Fig. 9 (e)), the thickest layer is coated when comparison in all the cases.

The thickness of the powder coating on the sample plate is increased with the number of the experimental analysis increasing, as shown in Fig. 10. In case of 1-3 layers coating, the trend graph of thickness is steeper than that case of 3-5 layers coating. The optimum value for the powder coating is 3-4 layers. The thickness increases when the number of powder coatings increases. From 2 to 5 layers, the thickness of the coating is increased by 0.75, 3.08, 4.63, and 5.60 times, respectively, when compared with the thickness of the coating in 1 layer. It can be seen that the thickness of the coating in cases of 3-4 layers is greater than in cases of 2-5 layers. By trend of thickness is steep in case of 3-4 layers.

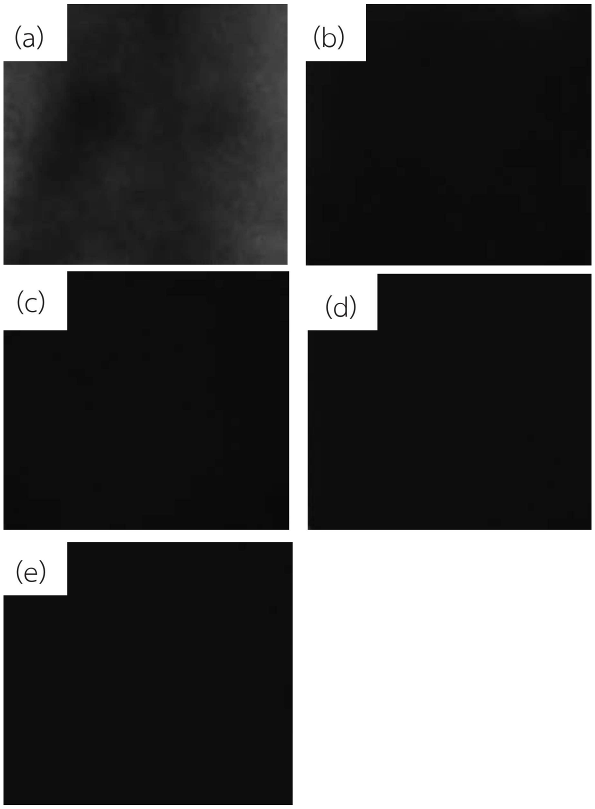

Fig. 9 Experimental results of powder coating on sample plate without electrostatic process (a) 1 layer (b) 2 layers (c) 3 layers (d) 4 layers (e) 5 layers

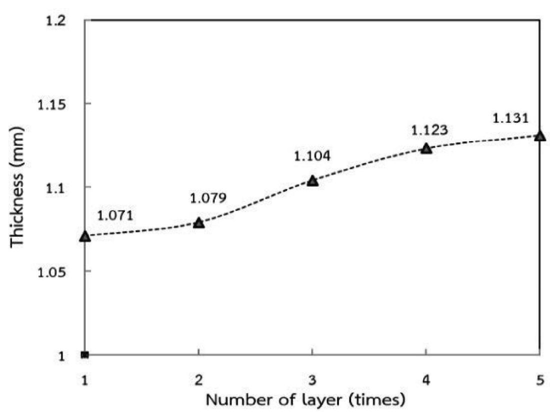

Fig. 10 Comparison between number of experimental analysis and thickness for powder coating on the sample plate without electrostatic process

4.3 Experimental study the powder coating on the sample with the electrostatic process

The electrode and the ground arrangement are studied for enhancement the electrostatic powder coating process. The powder coating is paint on the sample plate for 5 layers. The collected data of powder spray are investigated 3 times, and an average score is used for these experimental results. The diagram of the electrode and the ground arrangement are used from Fig. 1. The electrode and ground arrangements above the sample plate are composed of 7 patterns. Fig. 11 shows the powder coating on the sample with the electrostatic process in various the electrode and the ground arrangement. The powder coating on the sample with the electrostatic process from Fig. 11 (a-g) used the diagram from Fig. 1 (a-g), respectively.

The pattern 3 (Fig. 11 (c)) and the pattern 6 (Fig. 11 (f) show the electrode and the ground wire in the straight-line arrangements and the electrode and ground plate, respectively. These arrangements can support coating direction and coating process. This is because the electric charge can directly move from the electrode to the ground. The copper wire is supplied the electric current from the electrode and ground. It can be seen that the coatings can protect the substrate and the both patterns can control thickness. The pattern 4 (Fig. 11 (d)) and the pattern 6 (Fig. 11 (f)) show the electrode wire in the circle arrangement and the ground wire in the straight-line arrangement, respectively. The electrode wire is arranged in the circle and the square pattern so these arrangements cannot completely support coating direction and coating process. But the ground wire and ground circle can spread the electric charge so the most coating material is deposited on the sample plate. In case of ground point, the pattern 1 (Fig. 11 (a)), the pattern 2 (Fig. 11 (b)), and the pattern 7 (Fig. 11 (g)) show the electrode wire in the square arrangement, the electrode wire in the circle arrangement and the electrode wire in the square arrangement, respectively. These arrangements cannot support coating direction and coating process. Some coating material is deposited on the sample plate. In addition, the circle arrangement and the ground point are the unsuitable pattern. The electric charge is directly moved from the electrode wire to the ground point. This arrangement can abrupt the electrical discharge when a sufficiently high electric field creates an ionized, the electric spark is appeared, as shown in Fig. 10 (b). It can be seen that the damages of coating equipment are appeared the middle of the sample plate (ground point area).

For the electrostatic process in various the electrode and the ground arrangement, Fig. 12 shows the comparison between the thickness and the number of the experimental analysis for the powder coating on the sample plate. The thickness of the powder coating on the sample plate is increased with the number of the experimental analysis increasing. The results of Fig. 11 are the similar trend with the result of Fig. 12. In all the cases, the electrostatic process can more increase the thickness of coating than without the electrostatic process.

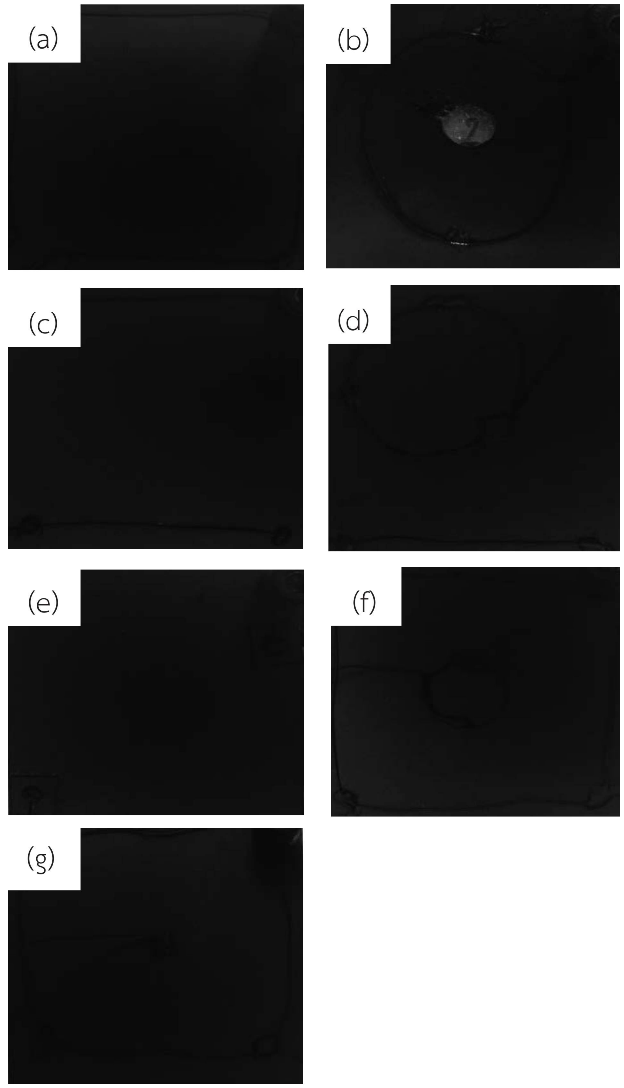

Fig. 11 The powder coating on the sample plate with the electrostatic process in various the electrode and the ground arrangement (a) pattern 1 (b) pattern 2 (c) pattern 3 (d) pattern 4 (e) pattern 5 (f) pattern 6 (g) pattern 7

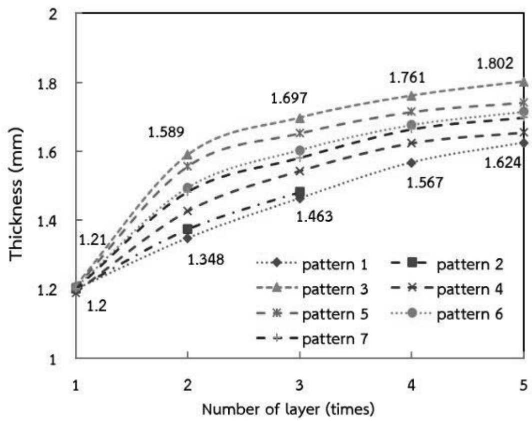

Fig. 12 Comparison between thickness and number of experimental analyses for the powder coating on the sample plate with the electrostatic process in various the electrode and the ground arrangement

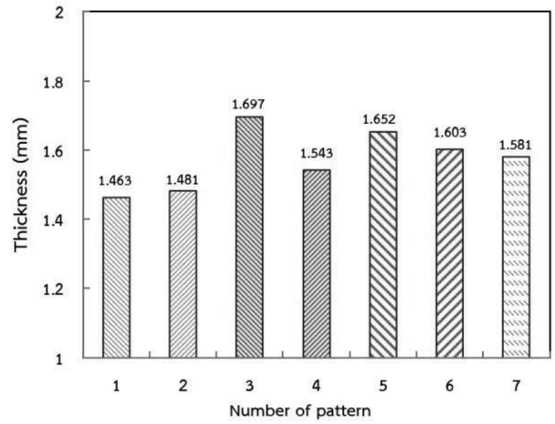

Fig. 13 The thickness of powder coating on sample plate with electrostatic process in various electrode and the ground arrangement for 3 layers

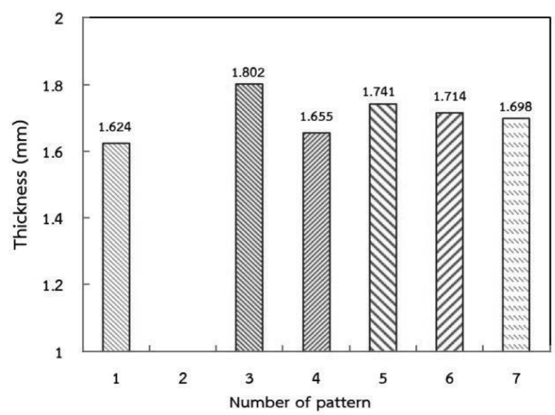

Fig. 14 The thickness of powder coating on sample plate with electrostatic process in various electrode and the ground arrangement for 5 layers

Fig. 13 and 14 show the thickness of the powder coating on the sample plate with the electrostatic process in various the electrode and the ground arrangement. The 7 patterns in various the electrode and the ground arrangement are used the data from Table 1 and Fig. 1. For 3 layers coating (Fig. 13), all of the patterns can be coated. The pattern 2 is not collect of data because the sample plate is damaged from the electric spark, as shown in 5 layers coating (Fig. 14).

The maximum coating is 5 layers, the thickness of powder coating for pattern 1 is 1.624 mm and the thickness of pattern 3-7 are 1.802 mm, 1.655 mm, 1.741 mm, 1.714 mm and 1.698 mm, respectively. The maximum of the powder coating on the sample plate with the electrostatic process is 1.59 times when comparing in without the electrostatic process.

4.4 Verification and problem statements for analysis

From a previous study, the electrode and the ground arrangement on the sample plate is the main influenced under the electrostatic powder coating process. The electrode and the ground arrangement are influenced with the maximum electric field, the maximum electric energy density and the maximum surface charge density so the electric force is differenced. The electric force under the electrostatic process is influenced with the impact pressure (P), impact velocity (v) and gravity force (F) so powder coating on the sample plate is differenced.

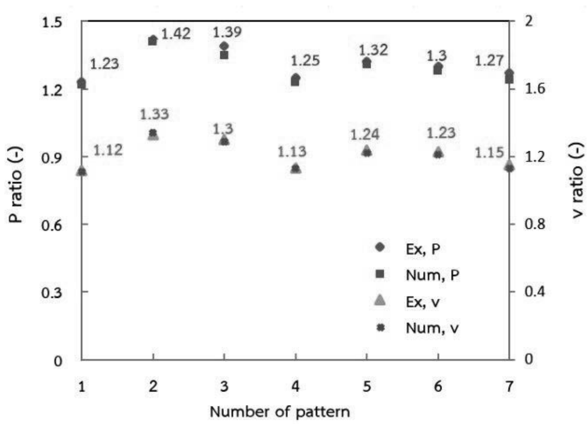

Fig. 15 The impact pressure ratio and the impact velocity ratio of powder coating in various electrode and the ground arrangement

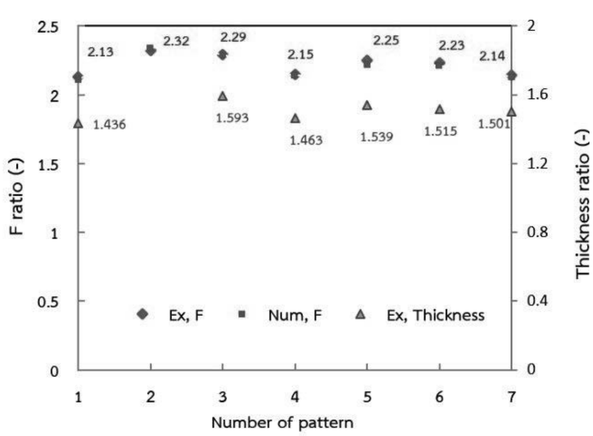

Fig. 16 The gravity force ratio and thickness ratio of powder coating in various electrode and the ground arrangement

Fig. 15 shows the impact pressure ratio (impact pressure with the electrostatic process per impact pressure without the electrostatic process; P ratio) and the impact velocity ratio (impact velocity with the electrostatic process per impact velocity without the electrostatic process; v ratio), respectively. Fig. 16 shows the gravity force ratio (gravity force with the electrostatic process per gravity force without the electrostatic process; F ratio) and thickness ratio (thickness of coating with the electrostatic process per thickness of coating without the electrostatic process; thickness ratio). In various electrode and the ground arrangement, the highest impact pressure ratio, the impact velocity ratio and gravity force ratio are the pattern 2 (electrode wire in circle arrangement and ground point) and pattern 3 (electrode and ground wire in straight line arrangement). The lowest impact pressure ratio, the impact velocity ratio and gravity force ratio are pattern 1 (electrode wire in square arrangement and ground point). From above numerical data, the maximum electric field, the maximum electric energy density and the maximum surface charge density in Fig. 6-8 are influenced in the electric force so it is affected with the impact pressure, impact velocity and gravity force in Fig. 15 and Fig. 16. From above experimental data, the all of patterns can be coated for 5 layers coating. The pattern 2 is not studied the data because the sample plate is damaged from the electric spark. The maximum and minimum of the powder coating on the sample plate with the electrostatic process are pattern 3 (electrode and ground wire in straight line arrangement) and pattern 1 (electrode wire in square arrangement and ground point), respectively. For Fig. 16, the thickness ratio of powder coating is the similar trend with the thickness of powder coating in Fig. 13.

The percent error is the difference between estimated value and the actual value in comparison to the actual value and is expressed as a percentage. From Fig. 15, the percentage error of the impact pressure ratio and the impact velocity ratio are 0.70-2.84% and 0.11-1.74%, respectively. From Fig. 16, the percentage error of the gravity force ratio 0-1.33%. From the above results, all the percentage error is lower than 3% so the data is generally accepted as being valid. It can be seen that numerical results had good agreement with experiment results.

5. Conclusion

The numerical and experimental result is carried out to study the influence of the coating process under the electrostatic process. The following are the conclusions of this research work:

1. The electric force is appearing under the electrostatic process, and the electrical voltage distribution is difference with various the electrode and ground arrangement.

2. The thickness of the powder coating on the sample plate is increased with the number of the coating, and the electrostatic process can more increase the thickness of coating than without the electrostatic process.

3. The electrode and ground arrangement are affected with the thickness of the powder coating on the sample plate.

6. Recommendation

All of parameter for coating should be observed during the coating operation so the idea behind this work can be used as guidance for special design for military vehicles and military aircraft coating material with the least manpower and minimum maintenance in the future.

7. Acknowledgements

This research was conducted at the Chulachomklao Royal Military Academy Fund and Department of Mechanical Engineering, Faculty of Engineering, Rajamangala University of Technology Rattanakosin for their support of this study.

8. References

(1) Fatemeh, S. M., Yong, C., Leonard, M. S. and Janusz, P. Optimization of the Coating Procedure for a High-Throughput 96-Blade Solid Phase Microextraction System Coupled with LC-MS/MS for Analysis of Complex Samples, Analytical Chemistry, Vol. 83, June 2011, pp. 6018-6025, (2011).

(2) Hamid, A., Sebastian, M. and Hamidreza, F. Effect of Interconnect Coating Procedure on Solid Oxide Fuel Cell Performance, Materials Letters, Vol. 259, Jam 2020, 126898, (2020).

(3) Klomkliang, P., Koedbankram, I., Abhaisuwan, S., Konpudsa, Y., Lamsee, M, Yochana, N., Punkla, T., Mawintorn, T. and Saneewong Na Ayuttaya, S. Effect of Inclined Plate under the Electrophoretic Deposition Technique for Coating Process. The 36th Conference of Mechanical Engineering Network of Thailand, July 2022, (2022).

(4) Kerry, N.A., Vinod, J.G., Gordon, P.B. and Victoria, J.G. Monitoring of a Military Vehicle Coating under Prohesion Exposure by Embedded Sensors, Progress in Organic Coating, Vol. 65(1), April 2009, pp. 142-151, (2009).

(5) Danqing, Z., Naiping, H. and Dale, W.S. Chapter 1 - Water-based Sol-Gel Coatings for Military Coating Applications, Handbook of Waterborne Coating, August 2020, pp. 1-27, (2020).

(6) Mehran, Q.M., Fazal, M.A., Bushroa, A.R. and Saeed, R. A Critical Review on Physical Vapor Deposition Coatings Applied on Different Engine Components, Critical Reviews in Solid State and Materials Sciences, Vol. 43(2), June 2017, pp. 158-175, (2018).

(7) Nina, S., Michael, T. and Christian, M. Hard Coatings for Cutting Applications: Physical vs. chemical Vapor Deposition and Future Challenges for the Coatings Community, Surface and Coating Technology, Vol. 429, January 2022, pp. 127949, (2022).

(8) Duhau, W. and Gordon, P.B. Sol-Gel Coatings on Metals for Corrosion Protection, Progress in Organic Coating, Vol. 64(4), March 2009, pp. 327-338, (2009).

(9) Lutz-Michael, B. Application of Hardmetals as Thermal Spray Coatings, International Journal of Refractory Metals and Hard Materials, Vol. 49, March 2015, pp. 350-364, (2015).

(10) Nina, S., Michael, T. and Christian, M. Hard Coatings for Cutting Applications: Physical vs. chemical Vapor Deposition and Future Challenges for the Coatings Community, Surface and Coating Technology, Vol. 429, January 2022, pp. 127949, (2022).

(11) Behzad, F., Navid, N. and Amir, D. On Coating Techniques for Surface Protection: A Review, Journal of Manufacturing and Materials Processing, Vol. 3(28), March 2019, pp. 1-22, (2019).

(12) S Sharmene, A., Base, T.E. and Inculet, I. Mathematical Modeling of Powder Paint Particle Trajectories in Electrostatic Painting, IEEE Transaction on Industry Application, Vol. 36(4), July-August 2000, pp. 992-997, (2000).

(13) Ye, Q., Steigleder, T., Scheibe, A. and Domnick, J. Numerical Simulation of the Electrostatic Powder Coating Process with a Corona Spray Gun, Journal of Electrostatics, Vol. 54(2), February 2002, pp. 189-205, (2002).

(14) Schmitt, C. and Lebienvenu, M. Electrostatic Painting of Conductive Composite Materials, Journal of Materials Processing Technology, Vol. 134(3), March 2003, pp. 303-309, (2003).

(15) Toljic, N., Adamiak, k., Castle, G.S.P., Kuo, H. and Fan, H. A full 3D Numerical Model of the Industrial Electrostatic Coating Process for Moving Targets, Journal of Electrostatics, Vol. 71(3), June 2013, pp. 299-304, (2013).

(16) Nobrega, J.H.C., Pio, P.G.C., Fernandes, G.L., Botelho, S.T. and Araujo, T.C. Sustainability in manufacturing processes: practices performed in metal forming, casting, heat treatment, welding and electrostatic painting, International Journal of Sustainable Development and World Ecology, Vol. 26(8), August 2019, pp. 684-697, (2019).

(17) Saneewong Na Ayuttaya, S. and Rattanadecho, P. Influence of Electrode Arrangements on Electrohydrodynamics and Transport Phenomenon within Water and Porous Samples Connected to Rectangular Duct. International Journal of Thermal Sciences, 130C, pp. 367-385, (2018).

(18) Saneewong Na Ayuttaya, S. A review of Electrohydrodynamics Application (Based on the Mechanism Characteristic). CRMA Journal, Vol. 15, December 2017, pp. 37-59, (2017).

(19) Shah. U., Zhu, J., Zhang, C. and Senior, J.H.N. Numerical Investigation of Coarse Powder and Air Flow in an Electrostatic Powder Coating Process, Powder Technology, Vol. 164(1), May 2006, pp. 22-32, (2006).

(20) David, J.G. Introduction to Electorhydrodynamics, Prentice Hall International, Inc., New Jersey, (1999).

(21) Landau, L.D. and Lifshitz, E.M. Electrohydrodynamics of Continuous Media. Pergamon, New York, (1963).

(22) Saneewong Na Ayuttaya, S., Chaktranond, C., Rattanadecho, P. and Kreewatcharin, T. Effect of Ground Arrangements on Swirling Flow in a Rectangular Duct Subjected to Electrohydrodynamic Effects. Journal of Fluids Engineering -Transactions of the ASME, Vol. 134, pp. 051211-9, (2012).